Chapter 16
Mapping Propulsive Efficiency of Flexible Bio-Inspired Fins

E. Paifelman, G. Costantino Muniz, S. Milana, A. Carcaterra, and E. Ciappi

Abstract This work presents a detailed parametric study of the propulsive performance of bio-inspired fish-like elastic fins through combined numerical modeling and experimental validation. The objective is to generate propulsion maps and identify the key parameters influencing propulsive efficiency, with direct implications for the design of efficient underwater propulsion systems. A fluid–structure interaction model is employed to predict the dynamic response of flexible fins across a wide range of material properties, stiffness levels, and geometric configurations. Extensive hydrodynamic channel tests have been conducted using a diverse set of fin prototypes, allowing systematic comparison with numerical predictions. The experimental data validate the model's accuracy and provide a rich dataset to assess thrust generation, elastic deformation, and efficiency under varying actuation conditions. The combined numerical-experimental analysis enables the creation of comprehensive propulsion maps, highlighting the sensitivity of performance to material and geometric parameters. The results offer valuable insights into the design space and establish a foundation for the optimization of future bio-inspired propulsion systems.

Keywords Fish-like · Bionspired robot · FSI model · Modal analysis · Biomimetic propulsion

Introduction

Biomimetic propulsion, inspired by fish locomotion, offers quiet operation, reduced risk in the event of contact with marine fauna, and high maneuverability characteristics that are particularly valuable for prolonged missions and operations in cluttered or sensitive habitats. Designing such systems, however, requires identifying which physical parameters most strongly govern thrust generation and efficiency, and understanding how these parameters interact across materials, geometries, and operating conditions. To address these needs, we combine a fluid–structure interaction (FSI) modeling framework with an experimental campaign aimed at mapping the propulsive response of flexible, fish-like fins representative of carangiform caudal propulsion. The numerical model enables dynamic simulations under controlled variations of stiffness distribution, plate geometry, and actuation, thereby exploring a design space relevant to marine robotics. The experimental activity in a water channel complements the simulations by validating trends and quantifying performance, using fin prototypes of different materials and thicknesses spanning both rigid and biomimetic stiffness ranges. In contrast to many previous studies focused on small propulsors [1, 2], we explicitly consider meter-scale platforms by employing plates of $500 \times 150\,[\mathrm{mm}]$, a size compatible with robotic bodies of about one meter in length and missions at significant depths. Methodologically, this work builds on our previous contributions to analytical hydroelastic modeling of oscillatory fish-like propulsion and to control strategies for systems with memory effects [3, 4, 5, 6, 7, 8, 9, 10, 11]. The outcome is a set of propulsion maps that synthesize the role of dimensionless stiffness, inertia ratio, reduced frequency, and Strouhal number, providing practical guidance for selecting materials and geometries and for tuning actuation to achieve efficient, scalable bio-inspired propellers suitable for real-world marine operations.

E. Paifelman · G. Costantino Muniz · E. Ciappi
National Research Council, Institute of Marine Engineering, Via di Vallerano 139, 00128 Rome, Italy
e-mail: elena.paifelman@cnr.it; gabriele.costantinomuniz@uniroma1.it; elena.ciappi@cnr.it

G. Costantino Muniz · S. Milana · A. Carcaterra
Sapienza University of Rome, Department of Aerospace and Mechanical Engineering, Via Eudossiana 18, 00184 Rome, Italy
e-mail: gabriele.costantinomuniz@uniroma1.it; silvia.milana@uniroma1.it; antonio.carcaterra@uniroma1.it

Kristin B. Zimmerman, PhD (eds.), *Structural Health Monitoring, Metamaterials, Metastructures and Additive Manufacturing and Dynamics of Biomedical and Bioinspired Systems, 2026, Vol. 10*, Conference Proceedings
of the Society for Experimental Mechanics Series, https://doi.org/10.1007/978-8-743-81449-8_16

Hydroelastic Modeling Framework

The two-way model developed to generate propulsion maps was obtained by coupling the one-dimensional Euler–Bernoulli plate equation with potential flow theory. This model represents the cross-section of the caudal fin and is generalized to handle non-rectangular shapes as well. The development and validation of the model, together with the formulation of the coupling terms (mass, stiffness, added damping, and memory effects) in closed form, are presented in detail in [3, 4]. The closed-form solution was derived using complex analysis, making the model semi-analytical [12]. Moreover, the model is formulated entirely in the time domain to allow integration with control logic [11, 10]. From this formulation, an integro-differential equation of motion was obtained, incorporating convolutional memory effects [8]. In this framework, Wu's theory is extended by replacing Theodorsen's frequency-dependent function with Wagner's time-dependent function. The caudal fin is thus modeled as a pitching/heaving Euler–Bernoulli beam subjected to two main external forces: one arising from pitch and heave accelerations, and the other of hydrodynamic origin. The hydrodynamic contribution accounts for both the non-circulatory and circulatory components, the latter associated with vortex shedding. The final modal equation of motion of the system is written as

$$\underline{\underline{\widetilde{M}}}\,\underline{\ddot{q}}(t) + \underline{\underline{\widetilde{C}}}\,\underline{\dot{q}}(t) + \underline{\underline{\widetilde{K}}}\,\underline{q}(t) + \left[\underline{\underline{\widetilde{\Psi}}}\,\ddot{\Phi}(t) + \underline{\underline{\widetilde{\Upsilon}}}\,\dot{\Phi}(t)\right] * \underline{q}(t) = \underline{\widetilde{F}} \tag{1}$$

Here, the matrices $\underline{\underline{\widetilde{M}}}$, $\underline{\underline{\widetilde{C}}}$, and $\underline{\underline{\widetilde{K}}}$ represent the effective mass, damping, and stiffness, including both structural and fluid contributions. Vortex shedding generates additional forces on the plate, described by the convolution matrices $\underline{\underline{\widetilde{\Upsilon}}}$ and $\underline{\underline{\widetilde{\Psi}}}$, which represent memory effects. Finally, the vector $\underline{\widetilde{F}}$ accounts for the external forces (see [3]).

Parametric Design maps

In order to properly design the propulsion system, it is necessary to consider multiple parameters simultaneously. Parametric maps provide an effective way to achieve this. Here, maps based on dimensionless stiffness $S = \frac{h_b^3 E}{\rho_f U_\infty^2 L^3}$ and solid-to-fluid inertia $R = \frac{\rho_s h_b}{\rho_f L}$ are proposed, both associated with the reduced frequency $\tilde{f} = f_\alpha L/U$. Since the system is intended to operate in an underwater environment, it is important that both R and S fall within the ranges observed in nature. Marine biology studies indicate that the efficiency of fish locomotion occurs for $R \ll 1$ and $10^{-3} < S < 10^3$ [13]. For this reason, our goal is to investigate these intervals, expanding the analysis to large geometries and engineering materials relevant for marine applications. The leading parameter for selecting the optimal configuration is the thrust coefficient

$$C_T = \frac{\bar{T}}{\frac{1}{2}\rho U^2 dL}.$$

However, optimal operation requires meeting two simultaneous conditions [14]. The first is that the actuation frequency f matches the first wet natural frequency of the panel f^1_{wet}, thereby inducing resonance and amplifying deformation. The second is that the Strouhal number $St = \frac{f_\alpha \chi}{U}$, with χ the peak-to-peak amplitude, falls within the range $[0.25 - 0.35]$. This ensures wake resonance and an increase in thrust production. When both conditions are satisfied, the motion is inherently efficient. A further requirement concerns the trailing edge velocity V_{TE}, which must satisfy $V_{TE} \ll U_\infty$ for the model to remain valid. An example of the maps is reported in Figure 1. All plate materials were experimentally characterized to ensure high fidelity of the numerical results. In the C_T maps, the white lines represent the boundaries of the optimal St range, while the magenta dots indicate the first wet frequencies of the tested plates. Optimal configurations are selected by restricting the candidate plates to those whose natural frequencies lie between the two white lines, thereby meeting the resonance and wake conditions. As shown, the ranges of both S and R fall within biomimetic values thanks to the combination of plate geometries and thicknesses employed. The lower row of Figure 1 also verifies the model validity, confirming that for the identified range of plates $U_\infty \approx 1\,[\mathrm{m/s}]$ and $V_{TE} < 0.6$, thus satisfying $V_{TE} \ll U_\infty$. Among all tested plates, the highest thrust coefficient $C_T = 0.27$ was obtained with a $3\,[\mathrm{mm}]$ HDPE plate. This procedure guided the selection of the most promising plate for the experimental campaign and the development of a first robotic prototype, which demonstrated encouraging results and supports further refinement of the proposed methodology.

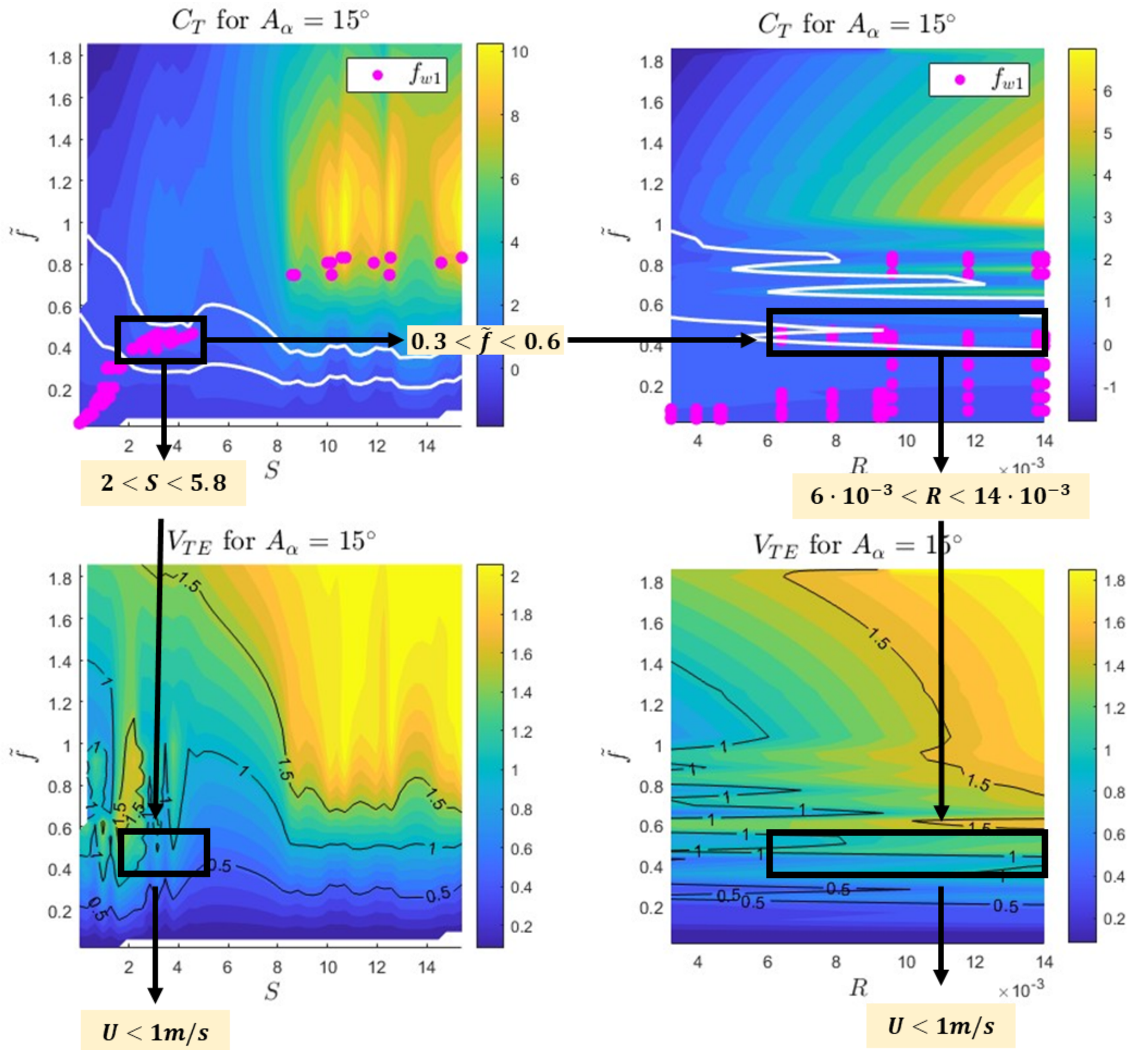

Fig. 1 Extraction of the best fin geometry using design maps. White lines indicate the boundaries of the optimal St range, while magenta dots mark the first wet frequencies of the tested plates

Experimental setup and validation

The experimental campaign is being conducted in the water channel of the Institute of Marine Engineering. The facility features a test section with a width of 536 $[mm]$ and a depth of 650 $[mm]$, allowing flow velocities of up to 1.8 $[m/s]$. The setup consists, from top to bottom, of a brushless Smartmotor (1.45 $[Nm]$ continuous torque, 3.39 $[Nm]$ peak torque, encoder resolution 8,000 [counts/rev], supporting DeviceNet, PROFIBUS, and CANopen communication protocols), connected to a planetary gearbox, a 6-axis load cell for measuring forces and moments (50 $[N]$, 5 $[Nm]$), and a rod to which the plates are attached (Figure 2). The system is closed by a flanged bushing at the bottom of the channel, acting as a flat hinge for the lower end of the rod. Because of vibrations caused by the water pumps, the setup is mounted on a structure designed to isolate the load cell and rod as much as possible. This significantly reduced noise in the force measurements, which are recorded using a Dewesoft acquisition system. In the lower part of the test section, beneath the plate, a window provides optical access for a Photron high-speed camera, enabling reconstruction of plate deformation during post-processing. The experimental campaign also investigates the influence of flow velocity. This parameter is controlled by varying the pump revolutions per minute and measuring the actual velocity with a Dantec Dynamics laser Doppler system. Tests were performed at different inflow speeds ($U_\infty = 0.1,\ 0.2,\ 0.4$ $[m/s]$) and pitching angles ($\alpha = 5°,\ 12.5°,\ 25°$). The plates tested so far include $2, 3$ $[mm]$ $HDPE$, $2, 3$ $[mm]$ $PMMA$, and $1, 2$ $[mm]$ aluminum plates. The actuation frequency was varied between 0.1 and 1.5 $[Hz]$, with each experiment repeated at least three times to ensure repeatability. This frequency range is

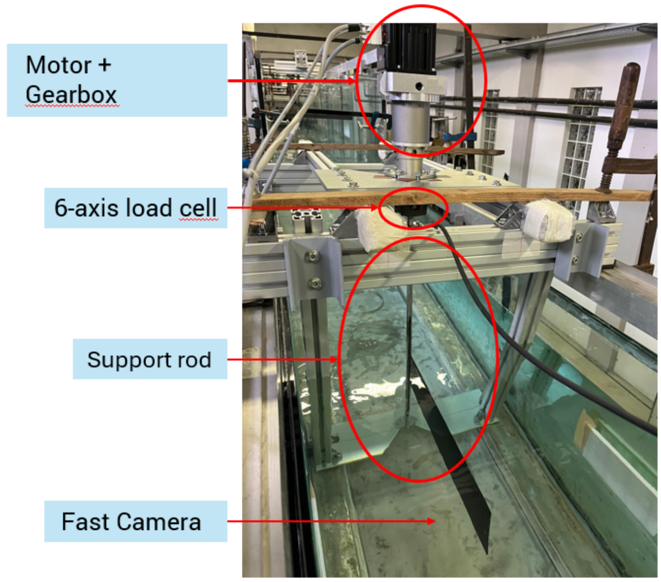

Fig. 2 Experimental setup with the 3 [mm] $HDPE$ plate

lower than that used in the numerical model, as the first wet frequency of all plates lies below 1.5 $[Hz]$, making it unnecessary to extend the range further. The experimental results are compared with the numerical predictions to assess the accuracy of the model. Figures 3a and 3b illustrate the case of the 3 $[mm]$ HDPE plate at $U_\infty = 0.1$ [m/s] and $\alpha = 12.5°$. The model provides an excellent approximation of both the peak-to-peak amplitude and the thrust production. However, both quantities are slightly overestimated at the first wet frequency of the system (dashed line), a discrepancy attributable to the modal nature of the model.

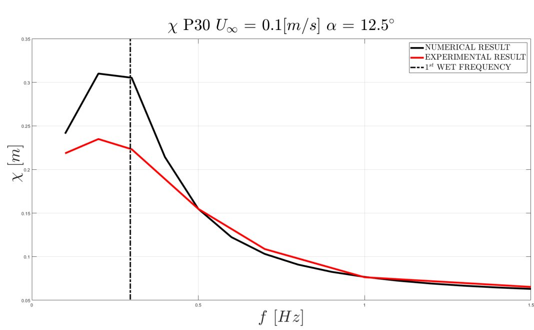

(a) Numerical (black) and experimental (red) comparison of peak-to-peak amplitude

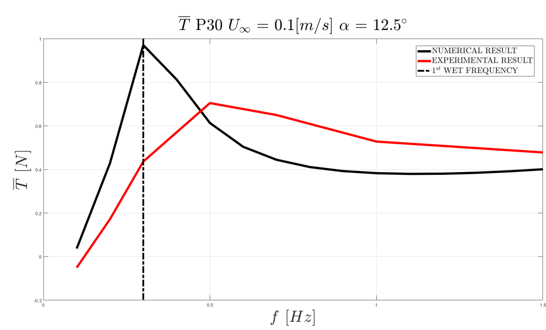

(b) Numerical (black) and experimental (red) comparison of thrust production

Fig. 3 Comparison between numerical and experimental results for the 3 $[mm]$ HDPE plate at $U_\infty = 0.1$ $[m/s]$ and $\alpha = 12.5°$. (a) Peak-to-peak amplitude. (b) Thrust production

Conclusions and Ongoing Work

The purpose of this article is to illustrate the tools we have developed to optimize the design of biomimetic propulsion systems. Starting from the development of a hydroelastic model, systematic simulations were performed and collected into maps to provide a synoptic view of thrust behavior as different parameters vary. This approach made it possible to identify the most efficient configuration in terms of thrust generation, which was then used as the starting point for the experimental campaign. The experimental tests validated the theoretical model, confirming the accuracy of the generated maps. Nevertheless, model updates are required to correct its behavior at low frequencies near the first wet resonance. To this end, additional experimental tests are currently being carried out to expand the parameter range and isolate the most influential factors. Furthermore, the introduction of corrective coefficients is being studied to compensate for the approximations inherent in the potential flow theory approach. Once updated and refined, the model will also be applied to investigate the effects of caudal fin shape and combined heaving–pitching motions, providing broader guidelines for designing optimal propellers for specific operating scenarios.

References

1. Kopman, V. and Porfiri, M. "Design, modeling, and characterization of a miniature robotic fish for research and education in biomimetics and bioinspiration". *IEEE/ASME Transactions on mechatronics*, 18(2):471–483 (2012)
2. Dewey, P.A., Boschitsch, B.M., Moored, K.W., Stone, H.A., and Smits, A.J. "Scaling laws for the thrust production of flexible pitching panels". *Journal of Fluid Mechanics*, 732:29–46 (2013)
3. Paifelman, E., Riccardi, G., and Ciappi, E. "Fluid-structure coupled analytical model for oscillatory fish-like propulsion". *Ocean Engineering*, 299:117292 (2024)
4. Paifelman, E., Milana, S., Culla, A., and Ciappi, E. "Swimming robot emulating fish propulsion". In *Proceedings of ISMA 2022 - International Conference on Noise and Vibration Engineering and USD 2022 - International Conference on Uncertainty in Structural Dynamics*, pages 3554–3563 (2022)
5. Paifelman, E., Pepe, G., and Carcaterra, A. "An optimal indirect control of underwater vehicle". *International Journal of Control*, 94(2):312–326 (2021)
6. Paifelman, E., Pepe, G., and Carcaterra, A. "Optimal control with memory effects: theory and application to wings". In *2019 18th European Control Conference (ECC)*, pages 319–324. IEEE (2019)
7. Paifelman, E., Pepe, G., La Gala, F., and Carcaterra, A. "Control of fluctuations of a tethered unmanned-underwater-vehicle". In *Proceedings of ISMA 2018-International Conference on Noise and Vibration Engineering and USD 2018-International Conference on Uncertainty in Structural Dynamics*, pages 241–251 (2018)
8. Pepe, G., Paifelman, E., and Carcaterra, A. "Feedback volterra control of integro-differential equations". *International Journal of Control*, 96(11):2651–2670 (2023)
9. Pepe, G., Paifelman, E., and Carcaterra, A. "Aeroelastic dynamic feedback control of a volterra airfoil". In *Advances in Nonlinear Dynamics: Proceedings of the Second International Nonlinear Dynamics Conference (NODYCON 2021), Volume 2*, pages 105–114. Springer International Publishing Cham (2022)
10. Pepe, G., Paifelman, E., Carcaterra, A., et al. "Optimal feedback control law for viscoelastic materials with memory effects". In *EURODYN...*, volume 1, pages 1445–1458. EASD Procedia (2020)
11. Pepe, G., Paifelman, E., Carcaterra, A., et al. "Volterra models of magnetorheological dampers and their application to vibrating systems". In *Proceedings of ISMA 2020-International conference on noise and vibration engineering and USD 2020-International conference on uncertainty in structural dynamics*, pages 817–826. KU Leuven-Departement Werktuigkunde (2020)
12. Carcaterra, A., Dessi, D., and Mastroddi, F. "Hydrofoil vibration induced by a random flow: a stochastic perturbation approach". *Journal of Sound and Vibration*, 283(1-2):401–432 (2005)
13. Smits, A.J. "Undulatory and oscillatory swimming". *Journal of Fluid Mechanics*, 874 (2019)
14. Triantafyllou, M., Triantafyllou, G., Gopalkrishnan, R., et al. "Wake mechanics for thrust generation in oscillating foils". *Physics of Fluids A Fluid Dynamics*, 3(12):2835 (1991)